

Article

Nonlinearity-Tolerant Probabilistically-Shaped Four-Dimensional Modulation at Spectral Efficiency of 9 Bits/Four-Dimensional Symbol

Pengpeng Wei ¹, Bo Song ^{2,*}, Yixin Zhang ^{3,4} and Xiang Li ^{5,*} ¹ School of Automation, China University of Geosciences, Wuhan 430074, China; weipp@cug.edu.cn² Beijing Institute of Space Science and Technology Information, Beijing 100072, China³ Key Laboratory of Intelligent Optical Sensing and Manipulation, Ministry of Education, Nanjing University, Nanjing 210093, China; zyixin@nju.edu.cn⁴ Institute of Optical Communication Engineering, College of Engineering and Applied Sciences, Nanjing University, Nanjing 210093, China⁵ School of Mechanical Engineering and Electronic Information, China University of Geosciences, Wuhan 430074, China

* Correspondence: imsongbo@163.com (B.S.); lix@cug.edu.cn (X.L.)

Abstract: Network traffic between data centers has grown rapidly in recent years. Therefore, an optical modulation format with high spectral efficiency is desired in inter-data center links at data rates of more than 400 Gb/s in each wavelength. In order to further improve the transmission performance in single-span inter-data center links, a nonlinearity-tolerant probabilistically-shaped 4D modulation format with a spectral efficiency of 9 bits/4D symbol is proposed. The proposed modulation format fills the gap between polarization-multiplexed 16- and 32-ary quadrature-amplitude modulation (PM-16QAM and PM-32QAM). In numerical simulations, we compare our proposed modulation format with probability-amplitude-shaped 64QAM (PAS-64QAM) and 512-set-partitioned 32QAM (512SP-32QAM) at a spectral efficiency of 9 bits/4D symbol in a single-span transmission link. The simulation results indicate that the proposed modulation format shows better linear and nonlinear performances than a 512SP-32QAM format. Compared with PAS-64QAM format, the proposed modulation format can provide similar transmission performance with improved fiber nonlinear tolerance.



Citation: Wei, P.; So, B.; Zhang, Y.; Li, X. Nonlinearity-Tolerant Probabilistically-Shaped Four-Dimensional Modulation at Spectral Efficiency of 9 Bits/4D-Symbol. *Photonics* **2023**, *10*, 865. <https://doi.org/10.3390/photonics10080865>

Received: 6 June 2023

Revised: 3 July 2023

Accepted: 19 July 2023

Published: 25 July 2023



Copyright: © 2023 by the authors. Licensee MDPI, Basel, Switzerland. This article is an open access article distributed under the terms and conditions of the Creative Commons Attribution (CC BY) license (<https://creativecommons.org/licenses/by/4.0/>).

1. Introduction

Due to the increasing traffic in inter-data-center networks, a high-capacity, single-span transmission system is desired. The current 400G ZR standard specifies a single-span transmission distance to be 120 km based on a uniformly distributed 16-quadrature amplitude modulation (QAM) format [1]. In order to further increase the data rate under the current constraints of a physical channel, a constellation-shaping technique has been considered to improve system performance [2]. The effectiveness of constellation shaping has been verified in the transmission of linear additive white Gaussian noise (AWGN) channels for QAM signals [2]. The theoretical analysis proves that constellation shaping can achieve a gain up to 1.53 dB over uniform QAM signaling [3,4]. In general, a shaping procedure tries to reduce the average transmitted power [3]. Currently, the most popular shaping scheme is based on probabilistic amplitude shaping (PAS), which is implemented in one dimension [4]. The advantages of PAS include the separation of shaping and coding operations, as well as the flexible adjustment of shaping entropy [5]. Several experimental demonstrations have proven that the performances of PAS-QAM signals based on Maxwell-Boltzmann (MB) distributions can approach the AWGN capacity [6–8].

However, PAS suffers from significant rate loss if the block length is short. A large block length can maximize the performance at the cost of heavy computational complex-

ity [9]. Moreover, transmission performances in fiber communication systems are not only affected by linear AWGN but also fiber nonlinear noise. It has been shown that the nonlinear effect of a fiber can significantly offset the performance improvement brought by PAS in a linear AWGN region. This is mainly because a one-dimensional MB distribution increases the power variation in a transmitted optical signal, resulting in more nonlinear noise [10]. It should be noted that fiber nonlinear impairments become dominant in the single-span transmission link when the accumulated chromatic dispersion value is low. Several nonlinear constellation-shaping schemes have been proposed to improve fiber nonlinear tolerance, such as nonlinear shell mapping [11], list-CCDM [12] and kurtosis-limited ESS schemes [13]. However, these schemes require additional memories and computational operations, resulting in high complexity and power consumption. In order to solve this problem, 4D modulation formats at 6 bits/4D symbol [14] and 7 bits/4D symbol [15] have been proposed to improve both linear and nonlinear performances. In order to achieve a data rate higher than 400 Gb/s, a higher spectral efficiency with more than 8 bits/4D symbol is required.

In this paper, we apply the concept of nonlinear shaping and propose a 4D shaping scheme considering both linear and nonlinear noise in fiber communication systems. We first study a conventional constant modulus 4D modulation format at a spectral efficiency of 6 bits/4D symbol (6b4D-12QAM) [14]. It is shown that constellation points of 6b4D-12QAM are non-uniformly distributed. Then, we design a 4D modulation format based on 32QAM with a targeted spectral efficiency (SE) of 9 bits/4D symbol, which is named “9b4D-32QAM”. The bit-to-symbol mapping scheme is optimized using the binary switch algorithm (BSA) [16]. Finally, we compare our designed 9b4D-32QAM with other known modulation formats with the same SE, including PAS-64QAM and 512-set-partitioned 32QAM (512SP-32QAM). It is shown that the designed 9b4D-32QAM can outperform PAS-64QAM and 512SP-32QAM in a single-span fiber transmission link in terms of both the optical signal-to-noise ratio (OSNR) margin and effective signal-to-noise ratio (SNR).

2. Constellation Design

In conventional 2D modulation, the optical amplitude and phase are modulated in each polarization. The optical signals in the two polarizations are independent. However, the 4D modulation considers the optical signal and phase in two polarizations jointly. 6b4D-12QAM with a constant modulus at an SE of 6 bits/4D symbol has been widely investigated in both simulations and experiments to show both the superior linear and nonlinear performance over polarization-multiplexed 8QAM (PM-8QAM) [14,17]. A typical 6b4D-12QAM can be viewed as a permutation of amplitudes [1 1 1 3] in two polarizations. The constellation points of 6b4D-12QAM with the corresponding probability distribution on a 2D plane are shown in Figure 1a. From Figure 1a, we can see that the occurrence rate of [1 1] is double of that of [1 3]. For example, if the signs of symbols in two polarizations are both set to positive, the possible constellations can then be [1 1 1 3], [1 1 3 1], [1 3 1 1], and [3 1 1 1]. This means the number of point 1 + j is 4, the number of point 1 + 3j is 2, and the number of point 3 + j is 2. Therefore, the constellation points of 6b4D-12QAM are non-uniformly distributed with probability shaped in four dimensions. In our view, both linear and nonlinear noise are considered in the constellation design of 6b4D-12QAM by applying probabilistic shaping and constant modulus 4D modulation techniques, respectively. The performances of 6b4D-12QAM have also been investigated via simulation and experimental demonstrations [14,17].

Following this concept, we shape the probability of the constellation points based on a 32QAM format to achieve an SE of 9 bits/4D symbol. The basic idea is to choose 512 4D permutations from the lowest power to the highest power among the total 1024 4D permutations [18]. By considering all 1024 4D permutations with different power levels, it is found that the number of 4D permutations with the five lowest power levels is exactly 512. In Table 1, the 512 signal points are listed by applying all permutations of coordinates and all

possible sign changes. The corresponding 2D probability distribution shown in Figure 1b also proves the non-uniform distribution of each constellation point. It is noted that the probability of constellation points with lower power is larger than the constellation points with higher power. Therefore, the average transmitted power is reduced, resulting in better tolerance to linear noise. It is also noted that the selected constellation points corresponding to the symbol power in two polarizations. Therefore, the lower symbol power variation in 4D may result in lower nonlinear noise [15].

Table 1. 4D constellation with 512 signal points.

Representative	$\frac{1}{4} \times \text{Power}$	$\frac{1}{16} \times \text{Number}$
[1 1 1 1]	1	1
[1 1 1 3]	3	4
[1 1 3 3]	5	6
[1 1 1 5]	7	4
[1 3 3 3]	7	4
[1 1 3 5]	9	12
[3 3 3 3]	9	1

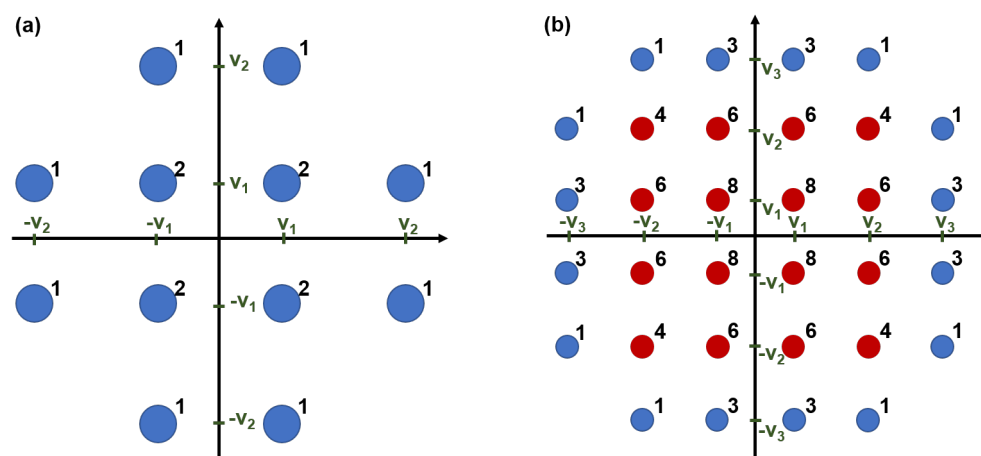


Figure 1. Probability distribution on 2D constellation for (a) 6b4D-12QAM in multiples of 1/2, and (b) 9b4D-32QAM in multiples of 1/128. The value of coordinates are given as $v_1 = 1, v_2 = 3, v_3 = 5$.

Bit-to-symbol mapping is another challenge issue related to the 4D modulation. Theoretically, the mapping could be found through exhaustive search. However, the computational complexity becomes intractable since $2^m!$ different possibilities have to be checked, where m represents the SE. In order to reduce the computational complexity, we apply the BSA to optimize the bit-to-symbol mapping. The basic idea of BSA is to switch the constellation points of two symbols to check whether the total cost is reduced. This process continues until no further reduction in the total cost is achieved. Several random initial mappings are required to realize the optimal mapping. Therefore, the optimization process is implemented to the whole number of possible symbols, which is 512 in our case. To further simplify the optimization process, we deliberately set the initial mapping by separating the constellation points into two parts, as shown in Figure 1b. Part I can be regarded as conventional 16QAM format. Therefore, the symbols indexed from 0 to 255 can be assigned according to Gray mapping rules of 4D-16QAM. Then, we pick up the indexes of symbol \mathfrak{R} , whose permutation of amplitudes can be expressed as [1, 1, 1, 3]. Next, we assign the corresponding permutation of amplitudes [1, 1, 1, 5] to the symbols with indexes $\mathfrak{R} + 256$. For example, the constellation points of symbol indexes 220 and 476 are assigned to be $[+1 + 1j, +1 + 3j]$ and $[+1 + 1j, +1 + 5j]$, respectively. Finally, we use BSA to optimize the mappings for permutation of amplitudes of [1, 1, 3, 5]. In this case, the initial mapping size

and the implemented number of possible symbols for switching are both reduced from 512 to 192. The cost function of BSA is given by

$$Cost = \sum_{i=1}^m \sum_{b=0}^1 \sum_{s_k \in \chi_b^i} \sum_{\bar{s}_k \in \chi_{\bar{b}}^i} |s_k - \bar{s}_k|^2 \quad (1)$$

where χ denotes a signal set of size 2^m , and $b \in [0, 1]$ and \bar{b} represent the bit inversion operation. The cost function in Equation (1) calculates the summation of square of Euclidean distance between any two symbols, whose Hamming distance is 1. The optimal bit-to-symbol mapping scheme (see in Appendix A) is assumed to be obtained after 1000 random initial mappings for the 192 signal points.

3. Numerical Analysis

In order to demonstrate the effectiveness of our proposed 4D modulation format, we conduct a simulation to investigate the single-span transmission performances in a five-channel wavelength division multiplexing (WDM) transmission system at Baud rate of 60 GBaud and 100 GHz channel spacing, as shown in Figure 2. The single-span transmission link is considered here because the nonlinear phase noise is dominated in such a link. The link is also targeted for inter-data-center communication and access network scenarios, which constitute the fastest growing section of the fiber communication market [19]. The simulation parameters are given in Table 2, which represents a typical fiber transmission system [20]. The propagation of the signal in the fiber link is simulated based on the Manakov equation. The central channel is assumed to be the channel of interest (COI). With the exception of the optical noise from the Erbium doped optical fiber amplifier (EDFA), additional optical noise is loaded to evaluate the system margin. We change the OSNR with excessive noise loading such that the target AIR is reached. In the simulation, three different modulation formats with SE of 9 bits/4D symbol are considered. The first one is the PAS-64QAM format with amplitude distribution of [0.5984, 0.3084, 0.0820, 0.0112] for a shaping length of 80 and [0.6276, 0.2980, 0.0672, 0.0072] for a shaping length of 5000. The second one is the proposed 9b4D-32QAM format. The third one is the 512SP-32QAM format, which is encoded by performing an XOR operation on the nine information bits to create one (the 10th) parity bit [21]. The digital signal processing is performed in a general flow including the chromatic dispersion compensation, the training symbol-aided 2×2 MIMO channel equalization and the decision-directed phase noise compensation. For the performance metrics [22], both achievable information rate (AIR) and effective SNR are considered, which are defined as:

$$AIR = H(X) - \sum_{i=1}^m H(B_i | Y) \quad (2)$$

$$SNR_{eff} = \frac{Var[X]}{Var[Y - X]} \quad (3)$$

where X are the transmitted symbols, Y are the received symbols after DSP. In our work, the AIR is calculated in 4D manner. Therefore, X and Y actually 2×1 vectors representing symbols in two polarizations. In Equation (2), $H(X)$ is the entropy of the transmitted symbol, which is 4.5 for all the modulation formats. B_i are the binary labels, and m represents the SE in 4D symbol, which is 9 in our work. $Var[\cdot]$ in Equation (3) represents the variance. It is noted that the rate loss is not considered in Equation (2). For PAS-64QAM with shaping length of 80, the rate loss should be considered for fair comparison.

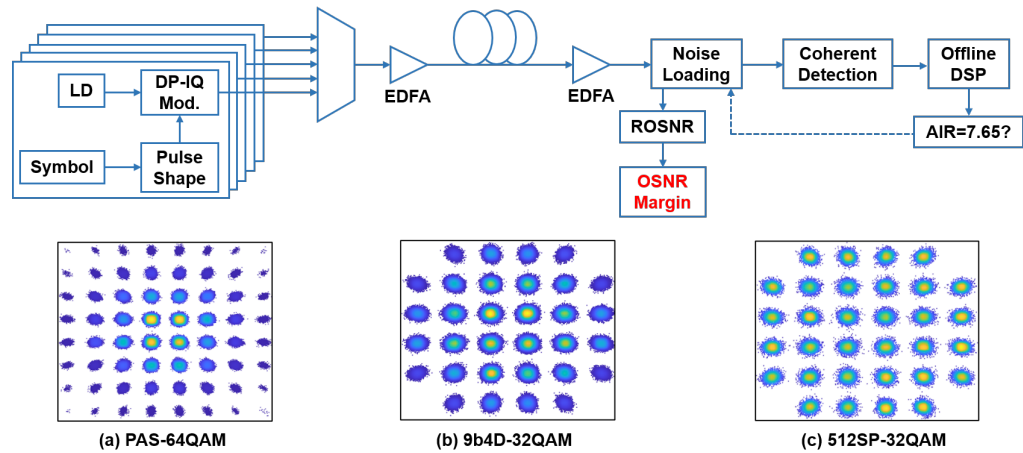


Figure 2. The Configuration of the simulated system and the procedure. Insets: constellations of (a) PAS-64QAM, (b) 9b4D-32QAM, (c) 512SP-32QAM.

Table 2. Simulation parameters.

Parameter	Value
Modulation	32 QAM and 64 QAM
Pol.-mux	yes
Symbol rate	60 GBd
WDM spacing	100 GHz
Pulse shape	root-raised cosine
Roll-off	0.1
Fiber length	120 km
Fiber loss	0.2 dB/km
Dispersion	16.7 ps/nm/km
Nonlinearity	1.3 1/W/km
EDFA noise figure	5 dB
Linewidth	100 kHz
Oversampling	×16
No. of simulation runs	10
QAM symbols per run	100,000

Figure 3 shows the back-to-back performance of the four modulation formats. Figure 3a shows AIR as a function of signal-to-noise ratio (SNR). In Figure 3a, the PAS-64QAM format has larger AIR than both 9b4D-32QAM formats. Specifically, the PAS-64QAM at length of 80 can provide a 0.53 dB gain over our proposed 9b4D-32QAM at AIR threshold of 7.65 bits/4D symbol. This is mainly because the amplitude distribution of PAS-64QAM is closer to the MB distribution. Another reason is related to the non-Gray mapping process of the 9b4D-32QAM, which may cause additional performance degradation. However, the proposed 9b4D-32QAM can provide gains of 0.51 dB over the traditional 512SP-32QAM at 7.65 bits/4D symbol. From Figure 3b, we can see that the difference in the effective SNR [23] is negligible among the four different modulation formats. This means that the designed constellations do not introduce a significant implementation penalty in the operating SNR region of interest.

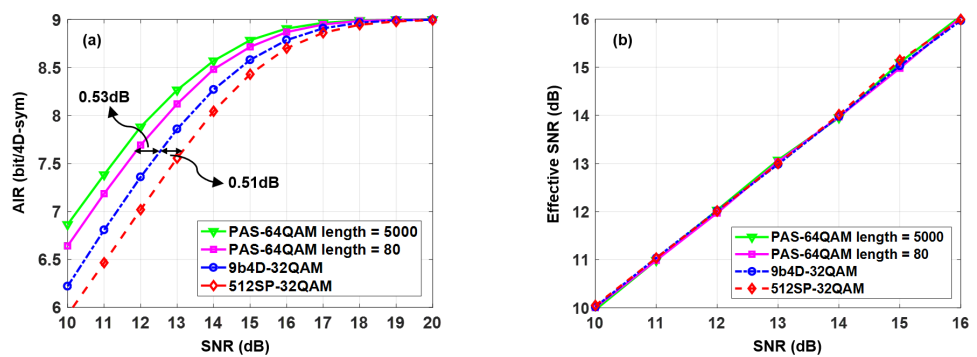


Figure 3. Back-to-Back performance of (a) AIR in bit/4D-sym versus SNR and (b) Effective SNR in dB versus SNR.

In our simulation, the single-span fiber transmission performance is evaluated by setting the OSNR to 30 dB/0.1 nm. As shown in Figure 4a, PAS-64QAM with shaping length of 5000 still has the largest AIR after fiber transmission, with a gain of 0.1 bit/4D sym over our proposed 9b4D-32QAM. However, both the proposed 9b4D-32QAM and PAS-64QAM with shaping length of 80 can achieve AIR of 8.22 bits/4D sym, which is 0.26 bit/4D sym higher than traditional 512SP-32QAM. This means that the proposed 9b4D-32QAM can achieve similar performances to the PAS-64QAM with lower computational complexity, since only a table look-up operation is required. The performance of effective SNR is shown in Figure 4b. It can be seen that the 9b4D-32QAM has the largest effective SNR after fiber transmission, which is 0.27 dB higher than the PAS-64QAM. It is also noted that the optimal launch power of the 9b4D-32QAM is 1 dB higher than the PAS-64QAM, which means the proposed 9b4D-32QAM can effectively mitigate the nonlinear noise after fiber transmission. The main reason is that the proposed 9b4D-32QAM signal only has five power levels in two polarizations, indicating lower power variation in the fiber transmission process. However, the 512SP-32QAM and PAS-64QAM have 9 and 21 power levels, resulting in larger power variation and fiber nonlinear noise.

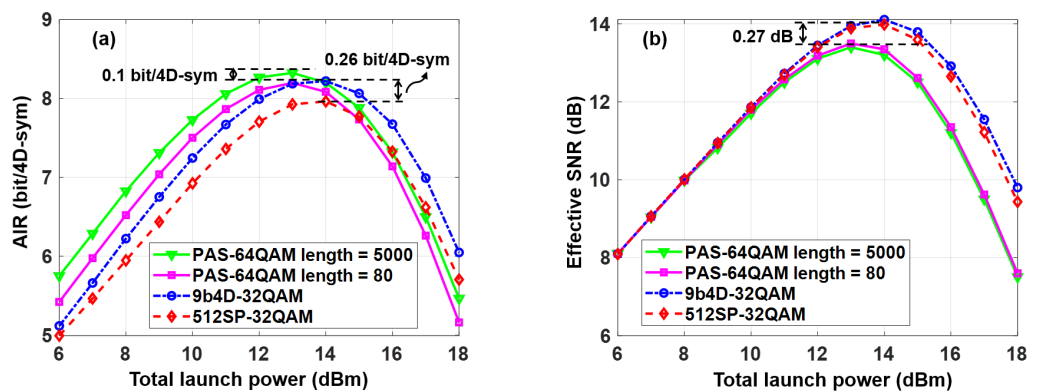


Figure 4. Performance of transmission over 120-km fiber link with OSNR of 30 dB/0.1 nm: (a) AIR in bit/4D-sym versus total launch power and (b) Effective SNR in dB versus total launch power.

Finally, we calculate the OSNR margin between the required OSNR to achieve 7.65 bits/4D sym and received OSNR, as shown in Figure 5. Although the PAS-64QAM with a shaping length of 5000 has the largest OSNR margin of 4.2 dB, the computational complexity is high at such a long shaping length. At the optimal launch power, the OSNR margin of the proposed 9b4D-32QAM is 4.05 dB, which is 0.15 dB and 0.55 dB higher than the PAS-64QAM with code length of 80 and the traditional 512SP-32QAM. It confirms that the proposed 9b4D-32QAM can improve both linear and nonlinear performance in a single-span fiber link.

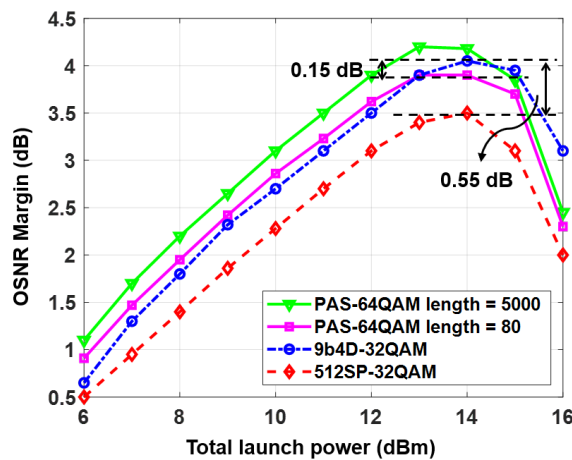


Figure 5. The OSNR margin versus the total launch power after single-span 120-km fiber link for the four modulation formats.

4. Conclusions

We propose and study a new 4D probabilistically shaped nonlinearity-tolerant modulation format with 9 bits/4D symbol, named 9b4D-32QAM. The bit-to-symbol mapping scheme is optimized based on the BSA. The proposed 9b4D-32QAM provides both linear gain, and improved effective SNR in the nonlinear region, enabling similar AIR performance as the PAS-64QAM with code length of 80 and superior performance over the 512SP-32QAM. For transmission over a single-span 120 km fiber link, an OSNR margin gains of 0.15 dB and 0.55 dB over the PAS-64QAM with a length of 80 and the traditional 512SP-32QAM are achieved. Compared with other constellation-shaping methods, the proposed 9b4D-32QAM signal has the advantages of low complexity operations and small look up table sizes. Considering the advantages and the performance improvement, the proposed 9b4D-32QAM format is desirable for future inter-data-center single-span fiber transmission networks at data rate of more than 400 Gb/s per wavelength. Future work may be related to the experimental demonstration in the WDM system to see how much performance improvement can be obtained if higher-order fiber nonlinear impairments are considered.

Author Contributions: Conceptualization, P.W. and X.L.; methodology, P.W.; software, P.W.; validation, P.W., B.S. and Y.Z.; formal analysis, P.W.; investigation, P.W.; writing—original draft preparation, P.W. and X.L.; writing—review and editing, B.S.; supervision, X.L.; project administration, X.L.; funding acquisition, Y.Z. All authors have read and agreed to the published version of the manuscript.

Funding: This is supported in part by the National Key R&D Program of China under Grant 2022YFB2903200, and in part by the Fundamental Research Funds for the Central Universities, No. 021314380211.

Institutional Review Board Statement: Not applicable.

Informed Consent Statement: Not applicable.

Data Availability Statement: The dataset used in this research is available upon valid request to any of the authors of this research article.

Conflicts of Interest: The authors declare no conflict of interest.

Appendix A

Table A1 lists the coordinates of the constellation points and the bit-to-symbol mapping of the proposed 9b4D-32QAM. The constellation is assumed to be normalized to $E_s = 2$, i.e., to unit energy per polarization.

Table A1. Coordinates and the bit-to symbol mapping of the proposed 9b4D-32QAM.

Coordinates				Labeling		Coordinates				Labeling		Coordinates				Labeling	
-0.82	0.82	-0.82	0.82	000000000	0.82	-0.82	0.82	-0.27	010101011	-0.27	0.27	-0.27	-1.36	101010110			
-0.82	0.82	-0.82	0.27	000000001	0.82	-0.82	0.27	0.82	010101100	-0.27	0.27	-0.82	-1.36	101010111			
-0.82	0.82	-0.82	-0.82	000000010	0.82	-0.82	0.27	0.27	010101101	-0.27	0.27	1.36	0.82	101011000			
-0.82	0.82	-0.82	-0.27	000000011	0.82	-0.82	0.27	-0.82	010101110	-0.27	0.27	1.36	0.27	101011001			
-0.82	0.82	-0.27	0.82	000000100	0.82	-0.82	0.27	-0.27	010101111	-0.27	0.27	1.36	-0.82	101011010			
-0.82	0.82	-0.27	0.27	000000101	0.82	-0.27	-0.82	0.82	010110000	-0.27	0.27	1.36	-0.27	101011011			
-0.82	0.82	-0.27	-0.82	000000110	0.82	-0.27	-0.82	0.27	010110001	-0.27	0.27	0.27	1.36	101011100			
-0.82	0.82	-0.27	-0.27	000000111	0.82	-0.27	-0.82	-0.82	010110010	-0.27	0.27	0.82	1.36	101011101			
-0.82	0.82	0.82	0.82	000001000	0.82	-0.27	-0.82	-0.27	010110011	-0.27	0.27	0.27	-1.36	101011110			
-0.82	0.82	0.82	0.27	000001001	0.82	-0.27	-0.27	0.82	010110100	-0.27	0.27	0.82	-1.36	101011111			
-0.82	0.82	0.82	-0.82	000001010	0.82	-0.27	-0.27	0.27	010110101	-0.27	-0.82	-1.36	0.27	101100000			
-0.82	0.82	0.82	-0.27	000001011	0.82	-0.27	-0.27	-0.82	010110110	-0.27	-1.36	-0.82	0.27	101100001			
-0.82	0.82	0.27	0.82	000001100	0.82	-0.27	-0.27	-0.27	010110111	-0.27	-0.82	-1.36	-0.27	101100010			
-0.82	0.82	0.27	0.27	000001101	0.82	-0.27	0.82	0.82	010111000	-0.27	-1.36	-0.82	-0.27	101100011			
-0.82	0.82	0.27	-0.82	000001110	0.82	-0.27	0.82	0.27	010111001	-0.27	-1.36	-0.27	0.82	101100100			
-0.82	0.82	0.27	-0.27	000001111	0.82	-0.27	0.82	-0.82	010111010	-0.27	-1.36	-0.27	0.27	101100101			
-0.82	0.27	-0.82	0.82	000010000	0.82	-0.27	0.82	-0.27	010111011	-0.27	-1.36	-0.27	-0.82	101100110			
-0.82	0.27	-0.82	0.27	000010001	0.82	-0.27	0.27	0.82	010111100	-0.27	-1.36	-0.27	-0.27	101100111			
-0.82	0.27	-0.82	-0.82	000010010	0.82	-0.27	0.27	0.27	010111101	-0.27	-0.82	1.36	0.27	101101000			
-0.82	0.27	-0.82	-0.27	000010011	0.82	-0.27	0.27	-0.82	010111110	-0.27	-1.36	0.82	0.27	101101001			
-0.82	0.27	-0.27	0.82	000010100	0.82	-0.27	0.27	-0.27	010111111	-0.27	-0.82	1.36	-0.27	101101010			
-0.82	0.27	-0.27	0.27	000010101	0.27	0.82	-0.82	0.82	010111110	-0.27	-1.36	0.82	-0.27	101101011			
-0.82	0.27	-0.27	-0.82	000010102	0.27	0.82	-0.82	-0.82	010111111	-0.27	-1.36	-0.82	0.27	101101012			
-0.82	0.27	-0.27	-0.27	000010111	0.27	0.82	-0.82	-0.27	010111110	-0.27	-1.36	-0.27	0.27	101101013			
-0.82	0.27	0.82	0.82	000011000	0.27	0.82	-0.82	-0.27	011000011	-0.27	-1.36	0.27	-0.82	101101110			
-0.82	0.27	0.82	0.27	000011001	0.27	0.82	-0.27	0.82	011000010	-0.27	-1.36	0.27	-0.27	101101111			
-0.82	0.27	0.82	-0.82	000011010	0.27	0.82	-0.27	0.27	011000011	-0.27	-0.27	-1.36	0.82	101110000			
-0.82	0.27	0.82	-0.27	000011011	0.27	0.82	-0.27	-0.82	011000010	-0.27	-0.27	-1.36	0.27	101110001			
-0.82	0.27	0.27	0.82	000011100	0.27	0.82	-0.27	-0.27	011000011	-0.27	-0.27	-1.36	-0.82	101110010			
-0.82	0.27	0.27	0.27	000011101	0.27	0.82	0.82	0.82	011000100	-0.27	-0.27	-1.36	-0.27	101110011			
-0.82	0.27	0.27	-0.82	000011110	0.27	0.82	0.82	0.27	011000101	-0.27	-0.27	-0.27	1.36	101110100			
-0.82	0.27	0.27	-0.27	000011111	0.27	0.82	0.82	-0.82	011000102	-0.27	-0.27	-0.82	1.36	101110101			
-0.82	-0.82	-0.82	0.82	000100000	0.27	0.82	0.82	-0.27	011000103	-0.27	-0.27	-0.27	-1.36	101110110			
-0.82	-0.82	-0.82	0.27	000100001	0.27	0.82	0.27	0.82	011000110	-0.27	-0.27	-0.27	-0.82	101110111			
-0.82	-0.82	-0.82	-0.82	000100010	0.27	0.82	0.27	0.27	011000111	-0.27	-0.27	-0.82	-1.36	101110112			
-0.82	-0.82	-0.82	-0.27	000100011	0.27	0.82	0.27	0.82	011000112	-0.27	-0.27	-0.82	-1.36	101110113			
-0.82	-0.82	-0.82	-0.82	000100100	0.27	0.82	0.27	0.27	011000113	-0.27	-0.27	-0.82	-1.36	101110114			
-0.82	-0.82	-0.82	-0.27	000100101	0.27	0.82	0.27	0.82	011000114	-0.27	-0.27	-0.82	-1.36	101110115			
-0.82	-0.82	-0.82	-0.82	000100110	0.27	0.82	0.27	0.27	011000115	-0.27	-0.27	-0.82	-1.36	101110116			
-0.82	-0.82	-0.82	-0.27	000100111	0.27	0.82	0.27	0.82	011000116	-0.27	-0.27	-0.82	-1.36	101110117			
-0.82	-0.82	-0.82	-0.82	000100010	0.27	0.82	0.27	0.27	011000117	-0.27	-0.27	-0.82	1.36	101110118			

Table A1. Cont.

Coordinates				Labeling		Coordinates				Labeling		Coordinates				Labeling	
-0.82	-0.82	-0.82	-0.27	000100011	0.27	0.82	0.27	-0.82	011001110	-0.27	-0.27	1.36	0.27	101111001			
-0.82	-0.82	-0.27	0.82	000100100	0.27	0.82	0.27	-0.27	011001111	-0.27	-0.27	1.36	-0.82	101111010			
-0.82	-0.82	-0.27	0.27	000100101	0.27	0.27	-0.82	0.82	011010000	-0.27	-0.27	1.36	-0.27	101111011			
-0.82	-0.82	-0.27	-0.82	000100110	0.27	0.27	-0.82	0.27	011010001	-0.27	-0.27	0.27	1.36	101111100			
-0.82	-0.82	-0.27	-0.27	000100111	0.27	0.27	-0.82	-0.82	011010010	-0.27	-0.27	0.82	1.36	101111101			
-0.82	-0.82	0.82	0.82	000101000	0.27	0.27	-0.82	-0.27	011010011	-0.27	-0.27	0.27	-1.36	101111110			
-0.82	-0.82	0.82	0.27	000101001	0.27	0.27	-0.27	0.82	011010100	-0.27	-0.27	0.82	-1.36	101111111			
-0.82	-0.82	0.82	-0.82	000101010	0.27	0.27	-0.27	0.27	011010101	0.27	0.82	-0.27	1.36	110000000			
-0.82	-0.82	0.82	-0.27	000101011	0.27	0.27	-0.27	-0.82	011010110	0.82	0.27	-0.27	1.36	110000001			
-0.82	-0.82	0.27	0.82	000101100	0.27	0.27	-0.27	-0.27	011010111	0.27	0.82	-0.27	-1.36	110000010			
-0.82	-0.82	0.27	0.27	000101101	0.27	0.27	0.82	0.82	011011000	0.82	0.27	-0.27	-1.36	110000011			
-0.82	-0.82	0.27	-0.82	000101110	0.27	0.27	0.82	0.27	011011001	0.82	1.36	-0.27	0.27	110000100			
-0.82	-0.82	0.27	-0.27	000101111	0.27	0.27	0.82	-0.82	011011010	1.36	0.82	-0.27	0.27	110000101			
-0.82	-0.27	-0.82	0.82	000110000	0.27	0.27	0.82	-0.27	011011011	0.82	1.36	-0.27	-0.27	110000110			
-0.82	-0.27	-0.82	0.27	000110001	0.27	0.27	0.27	0.82	011011100	1.36	0.82	-0.27	-0.27	110000111			
-0.82	-0.27	-0.82	-0.82	000110010	0.27	0.27	0.27	0.27	011011101	0.27	0.82	0.27	1.36	110000100			
-0.82	-0.27	-0.82	-0.27	000110011	0.27	0.27	0.27	-0.82	011011110	0.82	0.27	0.27	1.36	110000101			
-0.82	-0.27	-0.27	0.82	000110100	0.27	0.27	0.27	-0.27	011011111	0.27	0.82	0.27	-1.36	110000102			
-0.82	-0.27	-0.27	-0.27	000110101	0.27	-0.82	-0.82	0.82	0.82	011100000	0.82	0.27	0.27	-1.36	110000103		
-0.82	-0.27	-0.27	-0.82	000110110	0.27	-0.82	-0.82	0.27	011100001	0.82	1.36	0.27	0.27	110000110			
-0.82	-0.27	-0.27	-0.27	000110111	0.27	-0.82	-0.82	-0.82	011100010	1.36	0.82	0.27	0.27	110000111			
-0.82	-0.27	-0.27	0.82	000110110	0.27	-0.82	-0.82	-0.27	011100011	0.82	1.36	0.27	-0.27	110000112			
-0.82	-0.27	-0.27	0.27	000110111	0.27	-0.82	-0.82	0.27	011101111	0.27	0.82	0.27	-1.36	110000104			
-0.82	-0.27	-0.27	-0.82	000110110	0.27	-0.82	-0.82	-0.27	011101110	0.82	0.27	0.27	-1.36	110000105			
-0.82	-0.27	-0.27	-0.27	000110111	0.27	-0.82	-0.82	-0.27	011101111	0.82	1.36	0.27	-0.27	110000106			
-0.82	-0.27	-0.27	0.82	000111000	0.27	-0.82	-0.82	-0.27	011101100	0.82	1.36	0.27	-0.27	110000113			
-0.82	-0.27	-0.27	0.27	000111001	0.27	-0.82	-0.82	-0.27	011101100	1.36	0.82	0.27	-0.27	110000114			
-0.82	-0.27	-0.27	-0.82	000111010	0.27	-0.82	-0.82	-0.27	011101101	0.82	0.27	-0.27	-1.36	110000107			
-0.82	-0.27	-0.27	-0.27	000111011	0.27	-0.82	-0.82	-0.27	011101101	0.82	1.36	0.27	-0.27	110000108			
-0.27	0.82	-0.82	0.82	001000000	0.27	-0.82	0.82	-0.27	011101011	1.36	0.27	-0.27	-0.82	110010110			
-0.27	0.82	-0.82	0.27	001000001	0.27	-0.82	0.27	0.82	011101100	1.36	0.27	-0.27	-0.27	110010111			
-0.27	0.82	-0.82	-0.82	001000010	0.27	-0.82	0.27	0.27	011101110	1.36	0.27	-0.27	-0.27	110010100			
-0.27	0.82	-0.82	-0.27	001000011	0.27	-0.82	0.27	-0.82	011101110	1.36	0.27	0.82	0.27	110011001			
-0.27	0.82	-0.27	0.82	001000100	0.27	-0.82	0.27	-0.27	011101111	0.82	0.27	1.36	-0.27	110011010			
-0.27	0.82	-0.27	0.27	001000101	0.27	-0.82	-0.82	0.82	011101000	1.36	0.27	0.27	0.82	110011011			

Table A1. Cont.

Coordinates				Labeling		Coordinates				Labeling		Coordinates				Labeling	
−0.27	0.82	−0.27	−0.82	001000110	0.27	−0.27	−0.82	0.27	011110001	1.36	0.27	0.27	0.82	110011100			
−0.27	0.82	−0.27	−0.27	001000111	0.27	−0.27	−0.82	−0.82	011110010	1.36	0.27	0.27	0.27	110011101			
−0.27	0.82	0.82	0.82	001001000	0.27	−0.27	−0.82	−0.27	011110011	1.36	0.27	0.27	−0.82	110011110			
−0.27	0.82	0.82	0.27	001001001	0.27	−0.27	−0.27	0.82	011110100	1.36	0.27	0.27	0.27	−0.27	110011111		
−0.27	0.82	0.82	−0.82	001001010	0.27	−0.27	−0.27	0.27	011110101	0.27	−0.82	−0.27	1.36	110100000			
−0.27	0.82	0.82	−0.27	001001011	0.27	−0.27	−0.27	−0.82	011110110	0.82	−0.27	−0.27	1.36	110100001			
−0.27	0.82	0.27	0.82	001001100	0.27	−0.27	−0.27	−0.27	011110111	0.27	−0.82	−0.27	−1.36	110100010			
−0.27	0.82	0.27	0.27	001001101	0.27	−0.27	0.82	0.82	011111000	0.82	−0.27	−0.27	−1.36	110100011			
−0.27	0.82	0.27	−0.82	001001110	0.27	−0.27	0.82	0.27	011111001	0.82	−1.36	−0.27	0.27	110100100			
−0.27	0.82	0.27	−0.27	001001111	0.27	−0.27	0.82	−0.82	011111010	1.36	−0.82	−0.27	0.27	110100101			
−0.27	0.27	−0.82	0.82	001010000	0.27	−0.27	0.82	−0.27	011111011	0.82	−1.36	−0.27	−0.27	110100110			
−0.27	0.27	−0.82	0.27	001010001	0.27	−0.27	0.27	0.82	011111100	1.36	−0.82	−0.27	−0.27	110100111			
−0.27	0.27	−0.82	−0.82	001010010	0.27	−0.27	0.27	0.27	011111101	0.27	−0.82	0.27	1.36	110101000			
−0.27	0.27	−0.82	−0.27	001010011	0.27	−0.27	0.27	−0.82	011111110	0.82	−0.27	0.27	1.36	110101001			
−0.27	0.27	−0.27	0.82	001010100	0.27	−0.27	0.27	−0.27	011111111	0.27	−0.82	0.27	−1.36	110101010			
−0.27	0.27	−0.27	0.27	001010101	−0.27	0.82	−0.27	1.36	100000000	0.82	−0.27	0.27	−1.36	110101011			
−0.27	0.27	−0.27	−0.82	001010110	−0.82	0.27	−0.27	1.36	100000001	0.82	−1.36	0.27	0.27	110101100			
−0.27	0.27	−0.27	−0.27	001010111	−0.27	0.82	−0.27	−1.36	100000010	1.36	−0.82	0.27	0.27	110101101			
−0.27	0.27	0.27	0.82	001011000	−0.82	0.27	−0.27	−1.36	100000011	0.82	−1.36	0.27	−0.27	110101110			
−0.27	0.27	0.27	0.27	001011001	−0.82	1.36	−0.27	0.27	100000100	1.36	−0.82	0.27	−0.27	110101111			
−0.27	0.27	0.82	−0.82	001011010	−1.36	0.82	−0.27	0.27	100000101	0.82	−0.27	−1.36	0.27	110110000			
−0.27	0.27	0.82	−0.27	001011011	−0.82	1.36	−0.27	0.27	100000110	1.36	−0.27	−0.82	0.27	110110001			
−0.27	0.27	0.82	−0.27	001011011	−0.82	1.36	−0.27	−0.27	100000111	0.82	−0.27	−0.82	0.27	110110001			
−0.27	0.27	0.27	0.27	001011100	−1.36	0.82	−0.27	−0.27	100000111	0.82	−0.27	−1.36	−0.27	110110010			
−0.27	0.27	0.27	0.27	001011101	−0.27	0.82	0.27	1.36	100001000	1.36	−0.27	−0.82	−0.27	110110011			
−0.27	0.27	0.27	−0.82	001011110	−0.82	0.27	0.27	1.36	100001001	1.36	−0.27	−0.27	0.82	110110100			
−0.27	0.27	0.27	−0.27	001011111	−0.27	0.82	0.27	−1.36	100001010	1.36	−0.27	−0.27	0.27	110110101			
−0.27	−0.82	−0.82	0.82	001100000	−0.82	0.27	0.27	−1.36	100001011	1.36	−0.27	−0.27	−0.82	110110110			
−0.27	−0.82	−0.82	0.27	001100001	−0.82	1.36	0.27	0.27	100001100	1.36	−0.27	−0.27	−0.27	110110111			
−0.27	−0.82	−0.82	−0.82	001100010	−1.36	0.82	0.27	0.27	100001101	0.82	−0.27	1.36	0.27	110111000			
−0.27	−0.82	−0.82	−0.27	001100011	−0.82	1.36	0.27	−0.27	100001110	1.36	−0.27	0.82	0.27	110111001			
−0.27	−0.82	−0.82	0.27	001100100	−1.36	0.82	0.27	−0.27	100001111	0.82	−0.27	1.36	−0.27	110111010			
−0.27	−0.82	−0.27	0.27	001100101	−0.82	0.27	−1.36	0.27	100010000	1.36	−0.27	0.82	−0.27	110111011			
−0.27	−0.82	−0.27	−0.82	001100110	−1.36	0.27	−0.82	0.27	100010001	1.36	−0.27	0.27	0.82	110111100			
−0.27	−0.82	−0.27	−0.27	001100111	−0.82	0.27	−1.36	−0.27	100010010	1.36	−0.27	0.27	0.27	110111101			

Table A1. Cont.

Coordinates				Labeling		Coordinates				Labeling		Coordinates				Labeling	
-0.27	-0.82	0.82	0.82	001101000	-1.36	0.27	-0.82	-0.27	100010011	1.36	-0.27	0.27	-0.82	110111110			
-0.27	-0.82	0.82	0.27	001101001	-1.36	0.27	-0.27	0.82	100010100	1.36	-0.27	0.27	-0.27	110111111			
-0.27	-0.82	0.82	-0.82	001101010	-1.36	0.27	-0.27	0.27	100010101	0.27	0.82	-1.36	0.27	111000000			
-0.27	-0.82	0.82	-0.27	001101011	-1.36	0.27	-0.27	-0.82	100010110	0.27	1.36	-0.82	0.27	111000001			
-0.27	-0.82	0.27	0.82	001101100	-1.36	0.27	-0.27	-0.27	100010111	0.27	0.82	-1.36	-0.27	111000010			
-0.27	-0.82	0.27	0.27	001101101	-0.82	0.27	1.36	0.27	100011000	0.27	1.36	-0.82	-0.27	111000011			
-0.27	-0.82	0.27	-0.82	001101110	-1.36	0.27	0.82	0.27	100011001	0.27	1.36	-0.27	0.82	111000100			
-0.27	-0.82	0.27	-0.27	001101111	-0.82	0.27	1.36	-0.27	100011010	0.27	1.36	-0.27	0.27	111000101			
-0.27	-0.27	-0.82	0.82	001110000	-1.36	0.27	0.82	-0.27	100011011	0.27	1.36	-0.27	-0.82	111000110			
-0.27	-0.27	-0.82	0.27	001110001	-1.36	0.27	0.27	0.82	100011100	0.27	1.36	-0.27	-0.27	111000111			
-0.27	-0.27	-0.82	-0.82	001110010	-1.36	0.27	0.27	0.27	100011101	0.27	0.82	1.36	0.27	111001000			
-0.27	-0.27	-0.82	-0.27	001110011	-1.36	0.27	0.27	-0.82	100011110	0.27	1.36	0.82	0.27	111001001			
-0.27	-0.27	-0.27	0.82	001110100	-1.36	0.27	0.27	-0.27	100011111	0.27	0.82	1.36	-0.27	111001010			
-0.27	-0.27	-0.27	0.27	001110101	-0.27	-0.82	-0.27	1.36	100100000	0.27	1.36	0.82	-0.27	111001011			
-0.27	-0.27	-0.27	-0.82	001110110	-0.82	-0.27	-0.27	1.36	100100001	0.27	1.36	0.27	0.82	111001100			
-0.27	-0.27	-0.27	-0.27	001110111	-0.27	-0.82	-0.27	-1.36	100100010	0.27	1.36	0.27	0.27	111001101			
-0.27	-0.27	0.82	0.82	001111000	-0.82	-0.27	-0.27	-1.36	100100011	0.27	1.36	0.27	-0.82	111001110			
-0.27	-0.27	0.82	0.27	001111001	-0.82	-1.36	-0.27	0.27	100100100	0.27	1.36	0.27	-0.27	111001111			
-0.27	-0.27	0.82	-0.82	001111010	-1.36	-0.82	-0.27	0.27	100100101	0.27	0.27	-1.36	0.82	111010000			
-0.27	-0.27	0.82	-0.27	001111011	-0.82	-1.36	-0.27	-0.27	100100110	0.27	0.27	-1.36	0.27	111010001			
-0.27	-0.27	0.27	0.82	001111100	-1.36	-0.82	-0.27	-0.27	100100111	0.27	0.27	-1.36	-0.82	111010010			
-0.27	-0.27	0.27	0.27	001111101	-0.27	-0.82	0.27	1.36	100101000	0.27	0.27	-1.36	-0.27	111010011			
-0.27	-0.27	0.27	-0.82	001111110	-0.82	-0.27	0.27	1.36	100101001	0.27	0.27	-0.27	1.36	111010100			
-0.27	-0.27	0.27	-0.27	001111111	-0.27	-0.82	0.27	-1.36	100101010	0.27	0.27	-0.82	1.36	111010101			
0.82	0.82	-0.82	0.82	010000000	-0.82	-0.27	0.27	-1.36	100101011	0.27	0.27	-0.27	-1.36	111010110			
0.82	0.82	-0.82	0.27	010000001	-0.82	-1.36	0.27	0.27	100101100	0.27	0.27	-0.82	-1.36	111010111			
0.82	0.82	-0.82	-0.82	010000010	-1.36	-0.82	0.27	0.27	100101101	0.27	0.27	1.36	0.82	111011000			
0.82	0.82	-0.82	-0.27	010000011	-0.82	-1.36	0.27	-0.27	100101110	0.27	0.27	1.36	0.27	111011001			
0.82	0.82	-0.27	0.82	010000100	-1.36	-0.82	0.27	-0.27	100101111	0.27	0.27	1.36	-0.82	111011010			
0.82	0.82	-0.27	0.27	010000101	-0.82	-0.27	-1.36	0.27	100110000	0.27	0.27	1.36	-0.27	111011011			
0.82	0.82	-0.27	-0.82	010000110	-1.36	-0.27	-0.82	0.27	100110001	0.27	0.27	0.27	1.36	111011100			
0.82	0.82	-0.27	-0.27	010000111	-0.82	-0.27	-1.36	-0.27	100110010	0.27	0.27	0.82	1.36	111011101			
0.82	0.82	0.82	0.82	010001000	-1.36	-0.27	-0.82	-0.27	100110011	0.27	0.27	0.27	-1.36	111011110			
0.82	0.82	0.82	0.27	010001001	-1.36	-0.27	-0.27	0.82	100110100	0.27	0.27	0.82	-1.36	111011111			
0.82	0.82	0.82	-0.82	010001010	-1.36	-0.27	-0.27	-0.27	100110101	0.27	-0.82	-1.36	0.27	111100000			

Table A1. Cont.

Coordinates				Labeling		Coordinates				Labeling		Coordinates				Labeling	
0.82	0.82	0.82	-0.27	010001011	-1.36	-0.27	-0.27	-0.82	100110110	0.27	-1.36	-0.82	0.27	0.27	111100001		
0.82	0.82	0.27	0.82	010001100	-1.36	-0.27	-0.27	-0.27	100110111	0.27	-0.82	-1.36	-0.27	111100010			
0.82	0.82	0.27	0.27	010001101	-0.82	-0.27	1.36	0.27	100111000	0.27	-1.36	-0.82	-0.27	111100011			
0.82	0.82	0.27	-0.82	010001110	-1.36	-0.27	0.82	0.27	100111001	0.27	-1.36	-0.27	0.82	111100100			
0.82	0.82	0.27	-0.27	010001111	-0.82	-0.27	1.36	-0.27	100111010	0.27	-1.36	-0.27	0.27	111100101			
0.82	0.27	-0.82	0.82	010010000	-1.36	-0.27	0.82	-0.27	100111011	0.27	-1.36	-0.27	-0.82	111100110			
0.82	0.27	-0.82	0.27	010010001	-1.36	-0.27	0.27	0.82	100111100	0.27	-1.36	-0.27	-0.27	111100111			
0.82	0.27	-0.82	-0.82	010010010	-1.36	-0.27	0.27	0.27	100111101	0.27	-0.82	1.36	0.27	111101000			
0.82	0.27	-0.82	-0.27	010010011	-1.36	-0.27	0.27	-0.82	100111110	0.27	-1.36	0.82	0.27	111101001			
0.82	0.27	-0.27	0.82	010010100	-1.36	-0.27	0.27	-0.27	100111111	0.27	-0.82	1.36	-0.27	111101010			
0.82	0.27	-0.27	0.27	010010101	-0.27	0.82	-1.36	0.27	101000000	0.27	-1.36	0.82	-0.27	111101011			
0.82	0.27	-0.27	-0.82	010010110	-0.27	1.36	-0.82	0.27	101000001	0.27	-1.36	0.27	0.82	111101100			
0.82	0.27	-0.27	-0.27	010010111	-0.27	0.82	-1.36	-0.27	101000010	0.27	-1.36	0.27	0.27	111101101			
0.82	0.27	0.82	0.82	010011000	-0.27	1.36	-0.82	-0.27	101000011	0.27	-1.36	0.27	-0.82	111101110			
0.82	0.27	0.82	0.27	010011001	-0.27	1.36	-0.27	0.82	101000100	0.27	-1.36	0.27	-0.27	111101111			
0.82	0.27	0.82	-0.82	010011010	-0.27	1.36	-0.82	0.27	101000101	0.27	-0.27	-1.36	0.82	111110000			
0.82	0.27	0.82	-0.27	010011011	-0.27	1.36	-0.27	-0.82	101000110	0.27	-0.27	-1.36	0.27	111110001			
0.82	0.27	0.27	0.82	010011100	-0.27	1.36	-0.27	-0.27	101000111	0.27	-0.27	-1.36	-0.82	111110010			
0.82	0.27	0.27	0.27	010011101	-0.27	0.82	1.36	0.27	101001000	0.27	-0.27	-1.36	-0.27	111110011			
0.82	0.27	0.27	-0.82	010011110	-0.27	1.36	0.82	0.27	101001001	0.27	-0.27	-0.27	1.36	111110100			
0.82	0.27	0.27	-0.27	010011111	-0.27	0.82	1.36	-0.27	101001010	0.27	-0.27	-0.82	1.36	111110101			
0.82	-0.82	-0.82	0.82	010100000	-0.27	1.36	0.82	-0.27	101001011	0.27	-0.27	-0.27	-1.36	111110110			
0.82	-0.82	-0.82	0.27	010100001	-0.27	1.36	0.27	0.82	101001100	0.27	-0.27	-0.82	-1.36	111110111			
0.82	-0.82	-0.82	-0.82	010100010	-0.27	1.36	0.27	0.27	101001101	0.27	-0.27	1.36	0.82	111111000			
0.82	-0.82	-0.82	-0.27	010100011	-0.27	1.36	0.27	-0.82	101001110	0.27	-0.27	1.36	0.27	111111001			
0.82	-0.82	-0.82	0.82	010100100	-0.27	1.36	0.27	-0.82	101001111	0.27	-0.27	1.36	-0.82	111111010			
0.82	-0.82	-0.82	-0.27	010100101	-0.27	0.27	-1.36	0.82	101010000	0.27	-0.27	1.36	-0.27	111111011			
0.82	-0.82	-0.27	-0.82	010100110	-0.27	0.27	-1.36	0.27	101010001	0.27	-0.27	0.27	1.36	111111100			
0.82	-0.82	-0.27	-0.27	010100111	-0.27	0.27	-1.36	-0.82	101010010	0.27	-0.27	0.82	1.36	111111101			
0.82	-0.82	0.82	0.82	010101000	-0.27	0.27	-1.36	-0.27	101010011	0.27	-0.27	0.27	-1.36	111111110			
0.82	-0.82	0.82	0.27	010101001	-0.27	0.27	-0.27	1.36	101010100	0.27	-0.27	0.82	-1.36	111111111			
0.82	-0.82	0.82	-0.82	010101010	-0.27	0.27	-0.82	1.36	101010101	0.27	-0.27	0.82	-1.36	111111111			

References

1. OIF. 400G ZR Implementation Agreement. Available online: https://www.oiforum.com/wp-content/uploads/OIF-400ZR-01.0_reduced2.pdf (accessed on 10 March 2020).
2. Buchali, F.; Steiner, F.; Böcherer, G.; Schmalen, L.; Schulte, P.; Idler, W. Rate adaptation and reach increase by probabilistically shaped 64-QAM: An experimental demonstration. *J. Light. Technol.* **2016**, *34*, 1599–1609. [CrossRef]

3. Laroia, R.; Farvardin, N.; Tretter, S.A. On optimal shaping of multidimensional constellations. *IEEE Trans. Inform. Theory* **1994**, *40*, 1044–1056. [[CrossRef](#)]
4. Bocherer, G.; Steiner, F.; Schulte, P. Bandwidth efficient and rate-matched low-density parity-check coded modulation. *IEEE Trans. Commun.* **2015**, *63*, 4651–4665. [[CrossRef](#)]
5. Cho, J.; Chen, X.; Chandrasekhar, S.; Winzer, P. On line rates, information rates, and spectral efficiencies in probabilistically shaped QAM systems. *Opt. Exp.* **2018**, *26*, 9784–9791. [[CrossRef](#)] [[PubMed](#)]
6. Cho, J.; Chen, X.; Chandrasekhar, S.; Raybon, G.; Dar, R.; Schmalen, L.; Burrows, E.; Adamiecki, A.; Sell, S.C.; Pan, Y.; et al. Trans-atlantic field trial using probabilistically shaped 64-QAM at high spectral efficiencies and single-carrier real-time 250-Gb/s 16-QAM. In *Optical Fiber Communication Conference*; Optica Publishing Group: Washington, DC, USA, 2017; pp. 1–3.
7. Li, J.; Zhang, A.; Zhang, C.; Huo, X.; Yang, Q.; Wang, J.; Wang, J.; Qu, W.; Wang, Y.; Zhang, J.; et al. Field trial of probabilistic-shaping-programmable real-time 200-Gb/s coherent transceivers in an intelligent core optical network. In Proceedings of the 2018 Asia Communications and Photonics Conference (ACP), Hangzhou, China, 26–29 October 2018; pp. 1–3.
8. Maher, R.; Croussore, K.; Lauermann, M.; Going, R.; Xu, X.; Rahn, J. Constellation shaped 66 GBd DP 1024QAM transceiver with 400 km transmission over standard SMF. In Proceedings of the 2017 European Conference on Optical Communication (ECOC), Gothenburg, Sweden, 17–21 September 2017; pp. 1–3.
9. Amari, A.; Goossens, S.; Gültkin, Y.C.; Vassilieva, O.; Kim, I.; Ikeuchi, T.; Okonkwo, C.M.; Willems, F.M.; Alvarado, A.A. Introducing enumerative sphere shaping for optical communication systems with short blocklengths. *J. Light. Technol.* **2019**, *37*, 5926–5936. [[CrossRef](#)]
10. Tehrani, M.N.; Torbatian, M.; Sun, H.; Mertz, P.; Wu, K.-T. A novel nonlinearity tolerant super-gaussian distribution for probabilistically shaped modulation. In Proceedings of the 2018 European Conference on Optical Communication (ECOC), Rome, Italy, 23–27 September 2018; pp. 1–3.
11. Dar, R.; Feder, M.; Mecozzi, A.; Shtaif, M. On shaping gain in the nonlinear fiber-optic channel. In Proceedings of the 2014 IEEE International Symposium on Information Theory, Honolulu, HI, USA, 29 June–4 July 2014; pp. 2794–2798.
12. Wu, K.; Liga, G.; Sheikh, A.; Willems, F.M.J.; Alvarado, A. Temporal energy analysis of symbol sequences for fiber nonlinear interference modelling via energy dispersion index. *J. Light. Technol.* **2021**, *39*, 5766–5782. [[CrossRef](#)]
13. Gültkin, Y.C.; Alvarado, A.; Vassilieva, O.; Kim, I.; Palacharla, P.; Okonkwo, C.M.; Willems, F.M.J. Kurtosis-limited sphere shaping for nonlinear interference noise reduction in optical channels. *J. Light. Technol.* **2022**, *40*, 101–112. [[CrossRef](#)]
14. Chen, B.; Okonkwo, C.; Hafermann, H.; Alvarado, A. Polarization-ring-switching for nonlinearity-tolerant geometrically shaped four-dimensional formats maximizing generalized mutual information. *J. Light. Technol.* **2019**, *37*, 3579–3591. [[CrossRef](#)]
15. Chen, B.; Alvarado, A.; Heide, S.V.; den Hout, M.V.; Hafermann, H.; Okonkwo, C. Analysis and experimental demonstration of orthant-symmetric four-dimensional 7 bit/4D-sym modulation for optical fiber communication. *J. Light. Technol.* **2021**, *39*, 2737–2753. [[CrossRef](#)]
16. Schreckenbach, F.; Görtz, N.; Hagenauer, J.; Bauch, G. Optimization of symbol mappings for bit interleaved coded modulation with iterative decoding. *IEEE Commun. Lett.* **2003**, *7*, 593–595. [[CrossRef](#)]
17. Nakamura, T.; de Gabory, E.L.T.; Noguchi, H.; Maeda, W.; Abe, J.; Fukuchi, K. Long haul transmission of four-dimensional 64SP-12QAM signal based on 16QAM constellation for longer distance at same spectral efficiency as PM-8QAM. In Proceedings of the 2015 European Conference on Optical Communication (ECOC), Valencia, Spain, 27 September–1 October 2015; pp. 1–3.
18. Calderbank, A.R.; Ozarow, L.H. Nonequiprobable signaling on the Gaussian channel. *IEEE Trans. Inform. Theory* **1990**, *36*, 726–740. [[CrossRef](#)]
19. Geller, O.; Dar, R.; Feder, M.; Shtaif, M. A shaping algorithm for mitigating inter-channel nonlinear phase noise in nonlinear fiber systems. *J. Light. Technol.* **2016**, *34*, 3884–3889. [[CrossRef](#)]
20. Gan, Z.; Li, X.; Savory, S. Nonlinearity aware bisection-based sphere shaping for optical digital subcarrier multiplexing systems. *Opt. Exp.* **2022**, *30*, 44118–44131. [[CrossRef](#)] [[PubMed](#)]
21. Eriksson, T.A.; Sjödin, M.; Johannesson, P.; Andrekson, P.A.; Karlsson, M. Comparison of 128-SP-QAM and PM-16QAM in long-haul wdm transmission. *Opt. Exp.* **2013**, *21*, 19269–19279. [[CrossRef](#)] [[PubMed](#)]
22. Kojima, K.; Yoshida, T.; Koike-Akino, T.; Millar, D.S.; Parsons, K.; Pajovic, M.; Arlunno, V. Nonlinearity tolerant four-dimensional 2A8PSK family for 5–7 bit s/symbol spectral efficiency. *J. Light. Technol.* **2017**, *35*, 1383–1391. [[CrossRef](#)]
23. Skvortcov, P.; Phillips, I.; Forysiak, W.; Koike-Akino, T.; Kojima, K.; Parsons, K.; Millar, D.S. Nonlinearity tolerant LUT-based probabilistic shaping for extended-reach single-span links. *IEEE Photo. Technol. Lett.* **2020**, *32*, 967–970. [[CrossRef](#)]

Disclaimer/Publisher’s Note: The statements, opinions and data contained in all publications are solely those of the individual author(s) and contributor(s) and not of MDPI and/or the editor(s). MDPI and/or the editor(s) disclaim responsibility for any injury to people or property resulting from any ideas, methods, instructions or products referred to in the content.